Colloids and Surfaces A: Physicochem. Eng. Aspects 324 (2008) 149–154

Contents lists available at ScienceDirect

Colloids and Surfaces A: Physicochemical and Engineering Aspects

journal homepage: www.elsevier.com/locate/colsurfa

Aging mechanisms of oil-in-water emulsions based on a bioemulsifier produced by *Yarrowia lipolytica*

Joana R. Trindade[a], Mara G. Freire[a], Priscilla F.F. Amaral[b], Maria Alice Z. Coelho[b], João A.P. Coutinho[a], Isabel M. Marrucho[a,*]

[a] CICECO, Departamento de Química, Universidade de Aveiro, 3810-193 Aveiro, Portugal

[b] Departamento de Engenharia Bioquímica, Escola de Química, Universidade Federal do Rio de Janeiro, 31941-909 Rio de Janeiro, R.J., Brazil

ARTICLE INFO

Article history:
Received 28 November 2007
Received in revised form 17 March 2008
Accepted 8 April 2008
Available online 15 April 2008

Keywords:
Emulsion stability
Aging mechanisms
Yarrowia lipolytica
Yansan
Gum Arabic

ABSTRACT

The aging mechanisms of oil-in-water emulsions prepared with Yansan, a bioemulsifier produced by a Brazilian wild strain of *Yarrowia lipolytica*, IMUFRJ 50682, in glucose-based fermentation medium, were studied and compared with those prepared with Gum Arabic. Oil-in-water emulsions obtained by combining three different organic phases, perfluoro-*n*-hexane, *n*-hexadecane and toluene, with two aqueous buffers of different pH, and two bioemulsifiers, were studied through the evolution of the mean droplet size. The emulsions were prepared by sonication and their droplet size distribution was followed for 60 days at 301 K using image analysis. The results indicate that the aging mechanisms of the studied emulsions depend mainly on the bioemulsifier and on the pH of the medium. It is shown that the emulsions containing Gum Arabic age by coalescence while Yansan-based emulsions change their aging mechanisms from coalescence at pH 3 to molecular diffusion at pH 7.

1. Introduction

Bioemulsifiers have been recently attracting the industrial community as natural and promising candidates for the replacement of synthetic commercial surfactants due to their intrinsic properties such as lower toxicity, higher biodegradability, higher foaming capacity and higher activity at extreme temperatures, pH levels and salinity [1]. These compounds are biological molecules with surfactant properties similar to the well-known synthetic surfactants and include microbial compounds [2–5], natural polymers, such as Gum Arabic [5,6] which has been extensively exploited and used in the food industry as a surfactant agent, and other amphiphilic polymer surfactants usually based on polysaccharides, such as Emulsan [7–9] and Alasan [10–13]. So far, Gum Arabic is among the most studied and widely used hydrocolloid due to its excellent emulsifying capacity, ample spectrum of applications and millenary use [14].

Nowadays there is a wide range of commercial applications for bioemulsifiers such as oil recovery enhancement [15], bioremediation of oil-polluted soil and water [16], replacement of chlorinated solvents used in the cleaning up of oil-contaminated pipes [17], detergent industry [18], and formulation of oil-in-water emulsions in the food, biotechnological, pharmaceutical and cosmetic industries. The application of biodegradable and non-toxic bioemulsifiers can also be of substantial benefit in the biomedical and biotechnological fields. In particular, perfluorocarbon-based emulsions have been exploited as oxygen injectable carriers, as drug delivery systems or as cell culture media supplements [19,20]; and the employment of a non-toxic and biodegradable bioemulsifier may lead to further improvements of the technological specifications of such emulsions.

Clearly, if emulsions containing biosurfactants are to be used at the industrial level as carriers for active ingredients, they are required to have a long shelf-life. This means that they must not only be stable towards coalescence but also they cannot undergo significant Ostwald ripening or at least to ripen at an acceptable rate. Therefore, the study and evaluation of the aging mechanisms of oil-in-water emulsions containing biosurfactants is of special importance regarding their use in a large scale. Although many studies have been devoted to biosurfactants, they are often dedicated to their behaviour in semi-diluted aqueous solutions while surface-active properties are far less mentioned [13,21]. The few existent studies [13,21] concluded that Ostwald ripening is the main destabilization mechanism and that the nature of the disperse phase greatly affects the ripening rate.

Yansan was identified for the first time by our group in a previous work [5], in a glucose-based culture media of a wild strain of *Yarrowia lipolytica* in the absence of any water-immiscible

* Corresponding author. Tel.: +351 234 401 406; fax: +351 234 370 084.
E-mail address: imarrucho@ua.pt (I.M. Marrucho).

0927-7757/$ – see front matter
doi:10.1016/j.colsurfa.2008.04.009

substrates. This bioemulsifier is a glycoprotein complex and presents a high emulsification activity and stability in the pH range from 3.0 to 9.0 [5].

The main purpose of this study was to identify and understand the aging mechanisms of oil-in-water Yansan-based emulsions of three organic phases, perfluoro-*n*-hexane, *n*-hexadecane and toluene, and to infer about the pH influence on those. A comparison with the stability and aging mechanisms of emulsions composed by a commercial bioemulsifier of similar biochemical nature, such as Gum Arabic, was also carried to highlight similarities and differences between both surfactants and for a better understanding of the main phenomena taking place in the emulsions aging. The major cause of the organic phases employed is due to their relation with oil spills (hydrocarbons) and biotechnological applications (perfluorocarbons). The aging mechanisms of such composed emulsions were identified through image analysis [19].

2. Aging mechanisms

The emulsions physical degradation is due to the spontaneous trend towards a reduction in the Gibbs free energy, ΔG, achieved by reducing the size of the oil/water interface, A, and/or of the interfacial tension between the continuous and the dispersed phases, γ:

$$\Delta G = \gamma\,\Delta A - T\,\Delta S \tag{1}$$

Therefore, emulsion stability and associated aging mechanisms can be studied through the evolution of the mean droplet size and droplet size distribution. The increase of the droplet diameter is an indicator of the emulsion stability loss and the growth rate of the droplets indicates the mechanism responsible for their aging. Two main mechanisms have been proposed for the emulsions loss of stability: coagulation, followed by coalescence, and molecular diffusion [22].

Coalescence results from the formation of a larger droplet from the merging of smaller ones. Accordingly to the Van den Temple Theory [23], in coalescence, the cubic droplet radius (proportional to the droplet volume), $\bar{a}^3$, increases exponentially with time, t, from an initial average particle radius, $\bar{a}_0$, as described by the following equation:

$$\bar{a}^3 = \bar{a}_0^3 \exp(Kt) \tag{2}$$

where K is the coalescence constant.

The coarsening of emulsions through molecular diffusion mechanism, or Ostwald ripening mechanism, is characterized by the linear growth of the droplet volume with time without any contact between the individual particles. The molecular diffusion is a direct consequence of the Kelvin effect, where individual molecules tend to leave the smaller particles and diffuse through the continuous phase penetrating in larger droplets. The theoretical treatment known as the Lifshitz–Slyozov–Wagner (LSW) theory [24–27] states that the molecular diffusion can be characterized by the following equation:

$$\frac{\partial(\bar{a}^3)}{\partial t} = \frac{8CD\gamma V_{\mathrm{m}}^2}{9RT} \tag{3}$$

where C and D are, respectively, the solubility and the diffusion coefficient of the dispersed phase in the continuous medium, γ is the interfacial tension between the dispersed and the continuous phases, V_{m} is the molar volume of the dispersed phase, R is the usual gas constant and T is the absolute temperature.

According to Eq. (3) for oil-in-water emulsions, an increase in the particle's volume is proportional to the organic solubility in the aqueous phase, to the organic diffusion coefficient through the aqueous phase, and to the interfacial tension between the dispersed phase (organic phase) and the continuous phase (aqueous phase). Therefore, emulsions that undergo Ostwald ripening can be stabilized by decreasing at least one of these three factors.

3. Materials and experimental methods

3.1. Materials

The perfluoro-*n*-hexane (C_6F_{14}) was acquired at Fluorochem and *n*-hexadecane ($C_{16}H_{34}$) was from Sigma–Aldrich, both with purities ≥99%. Toluene (C_7H_8) was obtained from Panreac with a purity of ≥99.5%. The Gum Arabic was from Fluka and the Yansan was produced and purified as described elsewhere [5]. The organic solvents and the emulsifiers were used in the emulsions formulation without any further purification. Double distilled water, passed by a reverse osmosis system and further treated with a Milli-Q plus 185 purification apparatus, was employed in the preparation of the aqueous buffers (phosphate buffer for pH 7 and acetate buffer for pH 3).

3.2. Zeta potential

The electrokinetic zeta potential was measured, with a Coulter delsa 440SX, for both bioemulsifiers as a function of the pH, suspending 0.1 g of surfactant in 5 cm^3 of a KCl aqueous solution at an ionic strength of 0.001 mol dm^{-3}. At least eight independent measurements for each pH value were carried out and the respective standard deviations determined.

Table 1
Emulsions composition and optimal fitted equations for the mechanisms of stability loss for the studied emulsions ($\bar{a}^3$ = droplet diameter^3 (μm^3) and t = time (days))

Emulsion	Organic phase	Surfactant	Aqueous phase	Fitted equation
1	C_6F_{14} (30%, w/v)	Yansan	Phosphate buffer	$\bar{a}^3 = 0.1684t + 6.1357$
2	C_6F_{14} (15%, w/v)	Yansan	Phosphate buffer	$\bar{a}^3 = 0.3284t + 0.1064$
3	C_6F_{14} (15%, w/v)	Yansan	Acetate buffer	$\bar{a}^3 = 2.5755\,e^{0.0231t}$
4	C_6F_{14} (15%, w/v)	Gum Arabic	Phosphate buffer	$a^3 = 2.045\,0e^{0.0382t}$
5	C_6F_{14} (15%, w/v)	Gum Arabic	Acetate buffer	$\bar{a}^3 = 2.4748\,e^{0.0452t}$
6	$C_{16}H_{34}$ (30%, w/v)	Yansan	Phosphate buffer	$\bar{a}^3 = 0.1496t + 5.8851$
7	$C_{16}H_{34}$ (15%, w/v)	Yansan	Phosphate buffer	$a^3 = 0.3731t + 7.6170$
8	$C_{16}H_{34}$ (15%, w/v)	Yansan	Acetate buffer	$\bar{a}^3 = 11.6640\,e^{0.0155t}$
9	$C_{16}H_{34}$ (15%, w/v)	Gum Arabic	Phosphate buffer	$a^3 = 10.8177\,e^{0.0129t}$
10	$C_{16}H_{34}$ (15%, w/v)	Gum Arabic	Acetate buffer	$\bar{a}^3 = 11.3121\,e^{0.0143t}$
11	C_7H_8 (15%, w/v)	Yansan	Phosphate buffer	$a^3 = 0.0808t + 8.4780$
12	C_7H_8 (15%, w/v)	Yansan	Acetate buffer	$\bar{a}^3 = 6.8298\,e^{0.0102t}$
13	C_7H_8 (15%, w/v)	Gum Arabic	Phosphate buffer	$\bar{a}^3 = 7.8365\,e^{0.0081t}$
14	C_7H_8 (15%, w/v)	Gum Arabic	Acetate buffer	$\bar{a}^3 = 7.8044\,e^{0.0084t}$

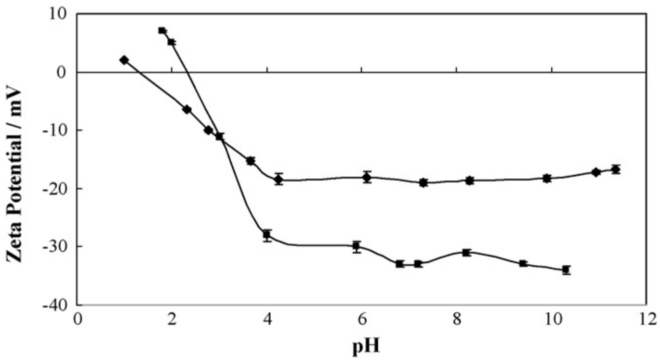

Fig. 1. Zeta potential as a function of the pH for Yansan (■) and Gum Arabic (♦) bioemulsifiers. Data markers represent the zeta potential average ± S.D.

3.3. Emulsions preparation

Oil-in-water emulsions were prepared with three individual organic phases, perfluoro-*n*-hexane, *n*-hexadecane and toluene, in combination with two bioemulsifiers, Gum Arabic and Yansan, to infer about the organic phase and surfactant influence in the aging mechanisms of such based emulsions. The effect of the organic phase concentration in the Yansan-based emulsions was also studied using two different concentrations, 15 and 30% (w/v), while maintaining the surfactant concentration constant, 0.6% (w/v). Since both surfactants are ionic, the effect of the medium pH in the emulsions stability was also addressed using standard buffers as the aqueous phase: an acetate buffer for pH 3 and a phosphate buffer for pH 7. The 10.0 cm^3 composition for each studied emulsion is described in Table 1. The emulsions were prepared by sonication, using a Sonics, Vibra Cell™ sonicator. The sonication was performed on two cycles of 2 min each, keeping the emulsion holder immerse in ice to prevent heating. Since 301 K is the optimal temperature for *Y. lipolytica*'s growth, this temperature was selected to perform the emulsion stability studies keeping the emulsions for 60 days in an air thermostatic oven (±0.5 K).

3.4. Image analysis

The emulsions droplets size and shape study was carried out during 60 days. For that purpose, optical microphotographs were taken with an Olympus optical microscope, model BX51, equipped with a digital camera. Each image was analyzed and the droplet size quantified with an image analysis program developed in Matlab® 6.1 for this purpose. A micrometer and appropriate software, Image-Pro® Plus 5.0, were used for the calibration of the droplet size. Further details about this procedure can be found elsewhere [19]. At each time an average of 100 droplets *per* image and about 10 different pictures from each sample were analyzed providing a total average of 1000 droplets for each point. The quantification step from image analysis [19] supplies a statistical analysis of the data providing the total number of analyzed objects, the average droplet diameter and its standard deviation as well as the particle size distribution. It also provides the particle roundness and its distribution, useful detecting if other objects than droplets are being analyzed.

4. Results and discussion

4.1. Bioemulsifiers characterization

The production and isolation of the Yansan bioemulsifier in the culture medium of *Y. lipolytica* IMUFRJ 50682, in the presence of glucose as the carbon source, was previously reported [5].

Surfactant molecules undergo self-association above a threshold concentration, CMC, to minimize the free energy of the self-assembled molecular structures as a whole. Yansan presents a CMC value (0.50 mg cm^{-3}) lower than that of Gum Arabic (1.65 mg cm^{-3}) [5], which means that the amount of Yansan required to solubilize organic compounds is smaller than for the commercial biopolymer.

The zeta potential of both bioemulsifiers was determined as a function of the pH and is compared in Fig. 1. It is shown that Yansan micelles present an acidic isoelectric point at *circa* pH 2.3 and negative charge on its surface, about −35 mV, for pH values higher than 4. On the other hand, Gum Arabic micelles present a more acidic isoelectric point at pH around 1.

4.2. Optimization of sonication time

In order to determine the optimum sonication time, the sonication was performed during two consecutive cycles of 1, 2 and 3 min. It was found that for sonication times longer than 4 min (two cycles of 2 min) the mean droplet diameter remains constant for the emulsion with *n*-hexadecane in phosphate buffer emulsified with Gum Arabic, and thus this time period was used for the preparation of all emulsions. The statistical analysis shows that the droplet size followed a Gaussian distribution and similar roundness was obtained for the three time periods tested.

4.3. Image analysis validation

The image analysis diameter results were compared and validated with the results obtained using a Zetasizer, from Malvern Instruments. For a Yansan-based perfluoro-*n*-hexane in acetate buffer emulsion after 20 days of aging, the image analysis resulted in an average droplet diameter of 1.9 ± 0.5 μm for 1076 analyzed

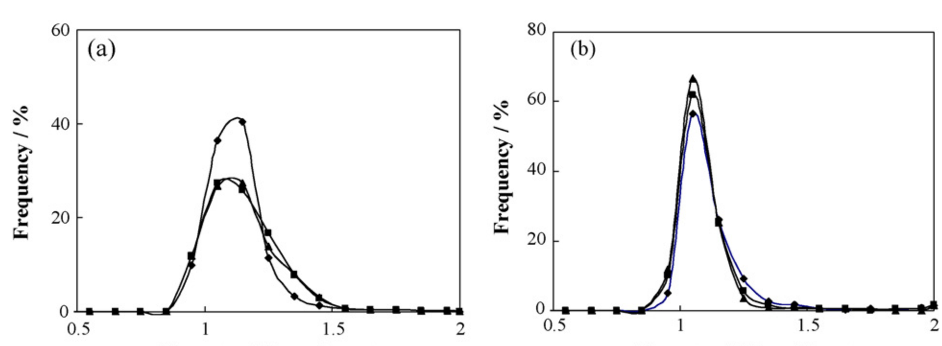

Fig. 2. Droplets size distribution for Emulsion 8: (a) (♦, 0 days; ■, 29 days; ▲, 57 days) and Emulsion 10: (b) (♦, 0 days; ■, 30 days; ▲, 53 days) at different periods of storage.

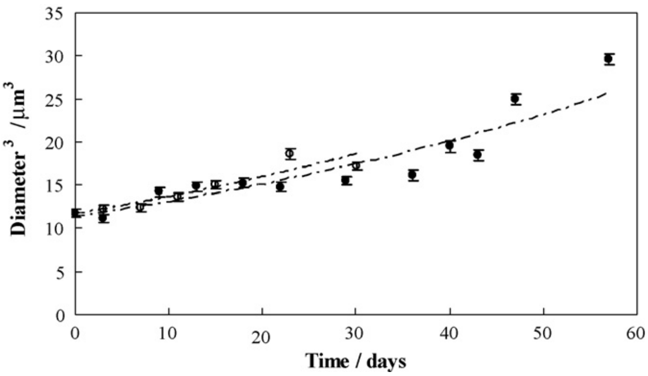

Fig. 3. Droplet size evolution as a function of time for *n*-hexadecane emulsions with pH 3 aqueous buffer and Yansan (○) or Gum Arabic (●). The dashed lines represent the coalescence mechanism. Data markers represent the droplet diameter^3 average ± uncertainty at a 99% confidence interval.

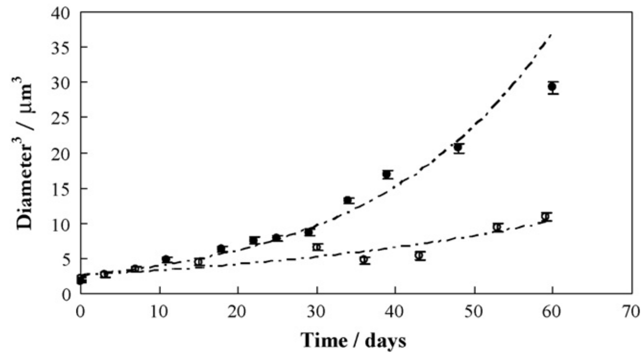

Fig. 5. Droplet size evolution as a function of time for perfluoro-*n*-hexane emulsions with pH 3 aqueous buffer and Yansan (○) or Gum Arabic (●). The dashed lines represent the coalescence mechanism. Data markers represent the droplet diameter^3 average ± uncertainty at a 99% confidence interval.

objects while the Zetasizer distribution indicated an average of 1.5 ± 0.4 µm for three independent readings of the same sample. The two methods are in agreement within their uncertainties and thus, the image analysis proved to be an appropriate method for studying the aging of these kinds of emulsions.

A statistical analysis of the experimental data aiming at assuring that no systematic errors (or bias) were made during the particle diameter measurements was also performed for all the samples. Among other issues, it is important to ensure that the program is detecting the smallest droplets and that the samples are randomly analyzed with no preferential droplet size detection. When no systematic errors are present, the population of all the studied emulsions follows a Gaussian distribution, as in the example depicted in Fig. 2 for Emulsions 8 and 10. Also note that these two examples show the scaling of the particle size distribution functions as expected from the LSW theory [24–27].

4.4. Emulsions stability and aging mechanisms

The results obtained for the particle size evolution with time and the respective uncertainty at a 99% confidence interval are presented in Figs. 3–10. The quantification procedure of the developed program provides the average droplets diameter and the respective standard deviation and from these the uncertainty at a 99% confidence level for the cubic droplet diameter was determined as described in the literature [28].

Eqs. (2) and (3) were used to correlate the experimental data and to identify the aging mechanisms associated to each emulsion. The correlations were chosen according to the best correlation factor of the fitted equation and are presented in Table 1. Besides the detection of the microscopically stability loss by the increase of the droplets size, at the end of 60 days of storage, the loss of stability of the emulsions by phase separation was also visible.

At both pH 3 and 7 and for all the organic phases studied, the Gum Arabic-based emulsions always loose stability by coalescence, while for Yansan-based emulsions two main mechanisms were identified: coalescence at pH 3 and molecular diffusion at pH 7. The fact that all the studied emulsions at pH 3 loose stability by coalescence can be explained by the proximity of the isoelectric point of both bioemulsifiers, indicating that the droplets surface charge is small and that particles can come together and coalesce. The pH not only affects the stability mechanism but also the growth rate of the emulsion droplets. For Gum Arabic-based emulsions the privileged mechanism is coalescence, independently of the pH or the oil phase employed. This finding suggests that these emulsions are predominantly stabilized by steric interactions, as changes in electrostatic interactions did not have a significant impact on droplet coalescence. Gum Arabic molecules present some cationic groups in the protein fraction of the molecule and, therefore, would be expected to become positively charged at pH lower than 1, as indicated by the zeta potential measurements.

The main difference in the aging mechanisms between the bioemulsifiers is observed at pH 7. The zeta potential measurements show that, at this pH, the Yansan molecules present a consider-

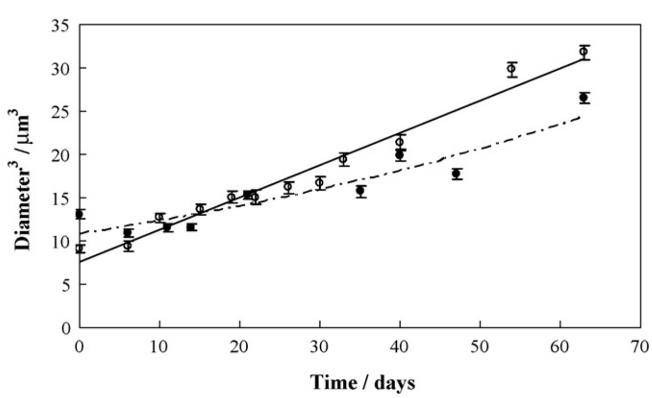

Fig. 4. Droplet size evolution as a function of time for *n*-hexadecane emulsions with pH 7 aqueous buffer and Yansan (○) or Gum Arabic (●). The dashed and the solid lines represent, respectively, the coalescence and the molecular diffusion mechanisms. Data markers represent the droplet diameter^3 average ± uncertainty at a 99% confidence interval.

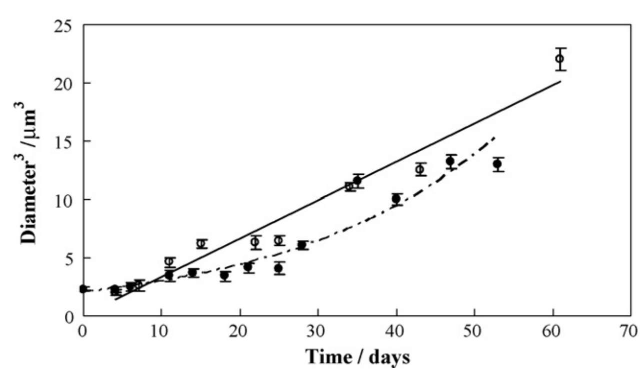

Fig. 6. Droplet size evolution as a function of time for perfluoro-*n*-hexane emulsions with pH 7 aqueous buffer and Yansan (○) or Gum Arabic (●). The dashed and the solid lines represent, respectively, the coalescence and the molecular diffusion mechanisms. Data markers represent the droplet diameter^3 average ± uncertainty at a 99% confidence interval.

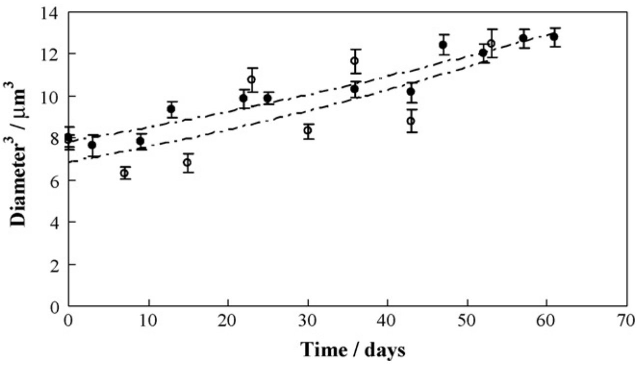

Fig. 7. Droplet size evolution as a function of time for toluene emulsions with pH 3 aqueous buffer and Yansan (○) or Gum Arabic (●). The dashed lines represent the coalescence mechanism. Data markers represent the droplet diameter^3 average ± uncertainty at a 99% confidence interval.

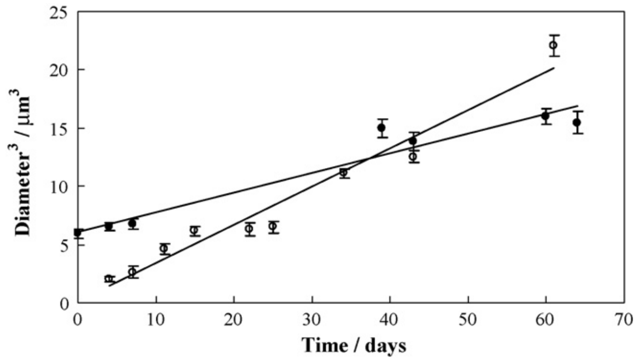

Fig. 9. Droplet size evolution as a function of time for Yansan emulsions with pH 7 aqueous buffer and perfluoro-*n*-hexane at 15% (w/v) (○) and 30% (w/v) (●). The solid lines represent the molecular diffusion mechanism. Data markers represent the droplet diameter^3 average ± uncertainty at a 99% confidence interval.

able negative surface charge and that the electrostatic repulsion does not allow the droplets to come sufficiently close to merge. The Yansan higher negative zeta potential values at pH 7 results from their higher protein content (15%, w/w) [5] and, therefore, a larger number of charged groups, when compared to Gum Arabic (2%, w/w) [29]. The carboxyl ions ($-COO^-$) are supposed to be at the periphery of the bioemulsifier molecules, since it is the main group that confers their amphiphilic character, and they are very active in creating an anionic environment, as observed for Yansan.

The influence of the organic phase can be inferred by the analysis of Figs. 4–8, which seems to indicate that the initial average particle size is dependent on the organic phase employed and independent of the pH. Note, however, that the emulsions were prepared in weight *per* volume which does not provide a very clear analysis, especially when the organic phases employed present different densities. Considering the densities of the organic phases at 298 K (perfluoro-*n*-hexane: 1.68 g cm^{-3} [30], toluene: 0.862 g cm^{-3} [31] and *n*-hexadecane: 0.770 g cm^{-3} [32]), it is simple to conclude that the emulsions prepared with perfluorocarbon at 30% (w/v) (17.9% v/v) have to be compared to those obtained for the 15% (w/v) emulsions with the other organic phases "17.4% (v/v) for toluene and 19.5% (v/v) for *n*-hexadecane". It can be observed that the initial average particle size for the Yansan-based emulsions prepared with the perfluorocarbon is similar to those obtained for the emulsions with *n*-hexadecane and toluene, although in the last case this parameter is a little higher than that for the other two organic phases.

The organic phase concentration influence in Yansan composed emulsions was studied with 15% (w/v) and 30% (w/v) of *n*-hexadecane and perfluoro-*n*-hexane at pH 7, as can be seen in Figs. 9 and 10. Fig. 9 compares the evolution of the average droplet size for Yansan and perfluoro-*n*-hexane-based emulsions at pH 7 for both organic phase concentrations. Fig. 10 depicts the average droplet size as a function of time for Yansan and *n*-hexadecane-based emulsions. It can be seen that the droplets initial average size of the perfluorocarbon emulsions increases by a factor of 2 with the concentration, while it remains unchanged for *n*-hexadecane composed emulsions. This results from the higher densities of perfluorocarbons when compared to hydrocarbons and from the higher surfactant availability as it was mentioned before [30]. The analysis of the stability mechanisms of these emulsions with both surfactants showed to be not affected by the organic phase concentration. Just an increase in the growth rate of the Ostwald ripening mechanism for *n*-hexadecane-based emulsions was observed, that is directly related with the hydrocarbon concentration and possible diffusion and mass transfer enhancement through the continuous phase.

At the same pH conditions and using the same surfactant there are no changes in the aging mechanisms due to the organic phase employed. However, a comparison between the growth rates of the several emulsions in Table 1 leads to the conclusion that, although the perfluoro-*n*-hexane-based emulsions provide the smallest droplets size, they also present the highest droplet growth rate when coalescence is the main mechanism. For example, for emulsions prepared with Yansan at pH 3 the values of 0.0102,

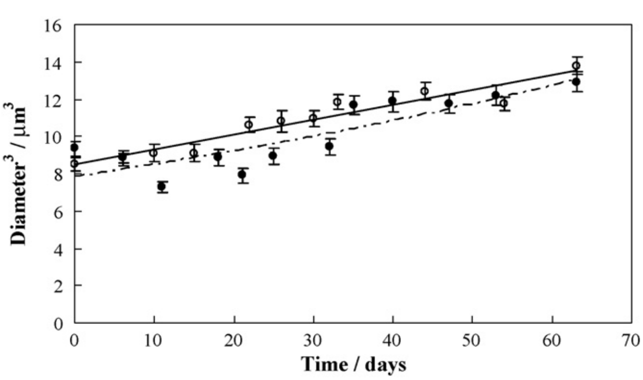

Fig. 8. Droplet size evolution as a function of time for toluene emulsions with pH 7 aqueous buffer and Yansan (○) or Gum Arabic (●). The dashed and the solid lines represent, respectively, the coalescence and the molecular diffusion mechanisms. Data markers represent the droplet diameter^3 average ± uncertainty at a 99% confidence interval.

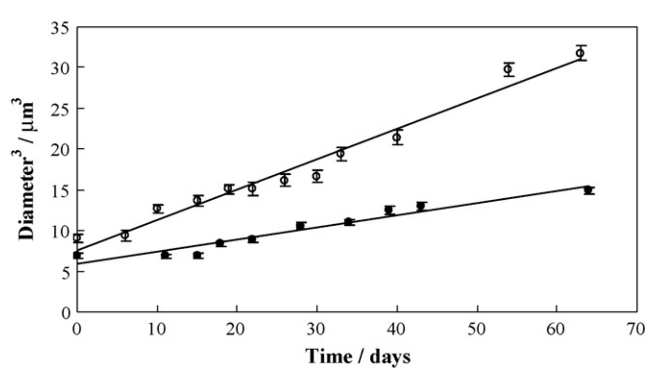

Fig. 10. Droplet size evolution as a function of time for Yansan emulsions with pH 7 aqueous buffer and *n*-hexadecane at 15% (w/v) (○) and 30% (w/v) (●). The solid lines represent the molecular diffusion mechanism. Data markers represent the droplet diameter^3 average ± uncertainty at a 99% confidence interval.

0.0155 and 0.0231 s^{-1} were obtained for toluene, *n*-hexadecane and perfluoro-*n*-hexane organic phases, respectively.

5. Conclusion

The aging mechanisms of oil-in-water emulsions prepared with Yansan, a bioemulsifier produced by a Brazilian wild strain of *Y. lipolytica*, IMUFRJ 50682, in glucose-based fermentation medium, were studied and compared with those prepared with Gum Arabic. The aging mechanisms of all emulsions studied are shown to be independent of the organic phase used in the emulsions formulation for a 60 days analysis. However, they were found to be dependent on the bioemulsifier and, for Yansan, also dependent on the medium pH. Gum Arabic-based emulsions always loose stability by coalescence, independently of all the other studied variables. Yansan-based emulsions change their stability loss mechanism from coalescence to molecular diffusion with the change of pH from 3 to 7, indicating that pH is the primary responsible for the stability of Yansan containing emulsions due to its high surface charge.

The results obtained here suggest that the bioemulsifier Yansan can be a future option for the oil industry in the process of cleaning of tanks, decontamination of polluted areas and in microbial-enhanced oil-recovery.

Acknowledgments

The authors thank financial support from Fundação para a Ciência e a Tecnologia (POCTI/EQU/44427/2002) and Ph.D. grant (SFRH/BD/14134/2003) of Mara G. Freire. The authors also thank financial support from GRICES/CAPES, CNPq and FAPERJ.

References

[1] I.M. Banat, I.M. Makkar, S.S. Cameotra, Appl. Microbiol. Biotechnol. 53 (2000) 495–508.
[2] M.C. Cirigliano, G.M. Carman, Appl. Environ. Microbiol. 48 (1984) 747–750.
[3] S.S. Zinjarde, A. Pant, J. Basic Microbiol. 42 (2002) 67–73.
[4] L.A. Sarubbo, C.B.B. Farias, G.M. Campos-Takaki, Curr. Microbiol. 54 (2007) 68–73.
[5] P.F.F. Amaral, M. Lehocky, J.M. da Silva, I.M. Marrucho, A. Barros-Timmons, M.A.Z. Coelho, J.A.P. Coutinho, Process Biochem. 41 (2006) 1894–1898.
[6] M.C. Cirigliano, G.M. Carman, Appl. Environ. Microbiol. 50 (1985) 846–850.
[7] J. Zhang, S.-H. Lee, R.A. Gross, D. Kaplan, J. Chem. Technol. Biotechnol. 74 (1999) 759–765.
[8] H. Bach, D.L. Gutnick, Appl. Microbiol. Biotechnol. 71 (2006) 177–183.
[9] H. Bach, Y. Berdichevsky, D. Gutnick, Appl. Environ. Microbiol. 69 (2003) 2608–2615.
[10] S. Navon-Venezia, E. Banin, E.Z. Ron, E. Rosenberg, Appl. Microbiol. Biotechnol. 49 (1998) 382–384.
[11] T. Barkay, S. Navon-Venezia, E.Z. Ron, E. Rosenberg, Appl. Environ. Microbiol. 65 (1999) 2697–2702.
[12] A. Toren, S. Navon-Venezia, E.Z. Ron, E. Rosenberg, Appl. Environ. Microbiol. 67 (2001) 1102–1106.
[13] J.D. Van Hamme, A. Singh, O.P. Ward, Biotechnol. Adv. 24 (2006) 604–620.
[14] J.I. Acedo-Carrillo, A. Rosas-Durazo, R. Herrera-Urbina, M. Rinaudo, F.M. Goycoolea, M.A. Valdez, Carbohydr. Polym. 65 (2006) 327–336.
[15] I.M. Banat, Biosource Technol. 51 (1995) 1–12.
[16] F. Volkering, A. Breure, W. Rulkens, Biodegradation 8 (1997) 401–417.
[17] A. Torem, S. Navon-Venezia, E.Z. Ron, E. Rosenberg, Appl. Environ. Microbiol. 67 (2001) 1102–1106.
[18] E. Rosenberg, E.Z. Ron, in: D.L. Kaplan (Ed.), Biopolymers from Renewable Resources, Springer, New York, 1998.
[19] M.G. Freire, A.M.A. Dias, M.A.Z. Coelho, J.A.P. Coutinho, I.M. Marrucho, J. Colloid Interface Sci. 286 (2005) 224–232.
[20] P.F.F. Amaral, M.G. Freire, M.H.M. Rocha-Leão, I.M. Marrucho, J.A.P. Coutinho, M.A.Z. Coelho, Biotechnol. Bioeng. 99 (2008) 588–598.
[21] V.M. Sadtler, P. Imbert, E. Dellacherie, J. Colloid Interface Sci. 254 (2002) 355–361.
[22] J. Sjoblom, Emulsion and Emulsion Stability, Surfactant Science Series, Marcel Dekker, New York, 1996.
[23] M. Van den Tempel, Recl. Trav. Chim. Pays-Bas 72 (1953) 433–442.
[24] I.M. Lifshitz, V.V. Slyozov, J. Phys. Chem. Solids 19 (1961) 35–50.
[25] C. Wagner, Z. Elektrochem. 65 (1961) 581–587.
[26] P. Taylor, Colloids Surf. A 99 (1995) 175–185.
[27] P.W. Voorhees, J. Stat. Phys. 38 (1985) 231–252.
[28] J.C. Miller, J.N. Miller, Statistics for Analytical Chemistry, 3rd ed., Elis Horwood Limited, Chichester, 1993.
[29] E. Dickinson, Food Hydrocolloids 17 (2003) 25–39.
[30] A.M.A. Dias, C.M.B. Goncalves, A.I. Caço, L.M.N.B.F. Santos, M.M. Piñeiro, L.F. Vega, J.A.P. Coutinho, I.M. Marrucho, J. Chem. Eng. Data 50 (2005) 1328–1333.
[31] A.J. Queimada, S.E. Quiñones-Cisneros, I.M. Marrucho, J.A.P. Coutinho, E.H. Stenby, Int. J. Thermophys. 21 (2003) 1221–1239.
[32] H.Y. Afeefy, J.F. Liebman, S.E. Stein, Neutral Thermochemical Data in NIST Chemistry WebBook, NIST Standard Reference Database Number 69, in: P.J. Linstrom, W.G. Mallard (Eds.), June 2005, National Institute of Standards and Technology, Gaithersburg MD, 20899 (http://webbook.nist.gov).